A High-Accuracy Finite Difference Scheme for Solving Reaction-Convection-Diffusion Problems with a Small Diffusivity

Po-Wen Hsieh[1], Suh-Yuh Yang[2,*] and Cheng-Shu You[2]

[1] *Department of Applied Mathematics, Chung Yuan Christian University, Jhongli City, Taoyuan County 32023, Taiwan*
[2] *Department of Mathematics, National Central University, Jhongli City, Taoyuan County 32001, Taiwan*

Abstract. This paper is devoted to a new high-accuracy finite difference scheme for solving reaction-convection-diffusion problems with a small diffusivity ε. With a novel treatment for the reaction term, we first derive a difference scheme of accuracy $\mathcal{O}(\varepsilon^2 h + \varepsilon h^2 + h^3)$ for the 1-D case. Using the alternating direction technique, we then extend the scheme to the 2-D case on a nine-point stencil. We apply the high-accuracy finite difference scheme to solve the 2-D steady incompressible Navier-Stokes equations in the stream function-vorticity formulation. Numerical examples are given to illustrate the effectiveness of the proposed difference scheme. Comparisons made with some high-order compact difference schemes show that the newly proposed scheme can achieve good accuracy with a better stability.

AMS subject classifications: 65N06, 65N12, 65N15, 76M20

Key words: Reaction-convection-diffusion equation, incompressible Navier-Stokes equations, boundary layer, interior layer, finite difference scheme.

1 Introduction

Let Ω be an open, bounded and convex polygonal domain in $\mathbb{R}^2$ with boundary $\partial\Omega$. We consider the following boundary value problem for the scalar reaction-convection-diffusion equation:

$$\begin{cases} -\varepsilon\Delta u + \boldsymbol{a}\cdot\nabla u + \sigma u = f & \text{in } \Omega, \\ u = g & \text{on } \partial\Omega, \end{cases} \quad (1.1)$$

*Corresponding author.
Email:* pwhsieh0209@gmail.com (P.-W. Hsieh), syyang@math.ncu.edu.tw (S.-Y. Yang), csdyou@gmail.com (C.-S. You)

where u is the physical quantity of interest (e.g., concentration of some chemical substance); $\varepsilon > 0$ is the diffusivity, which determines the size of diffusion relative to reaction or convection; $\boldsymbol{a} = (a_1(x,y), a_2(x,y))^\top$ is the given convection field; $\sigma \geq 0$ is the reaction coefficient; f is a given source term and g is the prescribed boundary data.

It was already known that the solution u of problem (1.1) may exhibit localized phenomena such as boundary and interior layers when the diffusivity ε is small enough compared with the size of convection field $\boldsymbol{a}$ or the reaction coefficient σ, i.e., the problem is reaction-convection-dominated. Boundary and interior layers are narrow regions in the domain Ω where the solution u changes rapidly. It is often difficult to resolve numerically the high gradients near the layer regions. However, the presence of layers in the solution is very common in many partial differential equations arising from physical science and engineering applications. Besides, problem (1.1) with a small diffusivity ε serves as a vehicle for the study of more advanced incompressible Navier-Stokes equations at high Reynolds numbers. Therefore, the reaction-convection-dominated case of problem (1.1) has been the focus of intense research for quite some time. Unfortunately, most conventional numerical methods for the reaction-convection-dominated problems are lacking in either stability or accuracy (cf. [14, 17, 23]). For example, when the mesh-Péclet number $Pe_h := \|\boldsymbol{a}\|_\infty h/(2\varepsilon)$ is large (it will occur if $0 < \varepsilon \ll 1$), the second-order central difference scheme performs very poorly since large spurious oscillations exhibit not only near the layer regions but also in the others; similar phenomena occur in the finite element method [2].

In this paper, we will focus on developing high-accuracy finite difference schemes for solving problem (1.1) with a small diffusivity ε. Although the usual upwind difference scheme is a simple and stable approach for solving problem (1.1), it exhibits a lower accuracy of $\mathcal{O}(h+k)$, where h and k denote the grid sizes in the x- and y-directions, respectively. On the other hand, higher-order finite difference approximations (that is, approximations whose errors are proportional to $\mathcal{O}(h^m + k^m)$ with $m > 2$) are possible, but they typically require non-compact stencils. A compact stencil utilizes eight grid points directly adjacent to the node about which the differences are taken for the discretization. Thus, the use of non-compact stencils complicates numerical formulations near boundaries, increases matrix bandwidth and hence the computational cost. In [20], Spotz proposed a class of fourth-order finite difference schemes that do not look at extra points, but instead approximate the leading terms in the truncation error to obtain higher accuracy. This is achieved by differentiating the governing equation to find, for example, the third derivative in terms of lower-order derivatives that can then be differenced compactly and included in the finite difference formulation. This increases the accuracy while still maintaining an overall compact stencil. However, a more careful calculation shows that the accuracy of the fourth-order compact difference schemes is indeed $\mathcal{O}((h^4 + k^4)/\varepsilon)$ and then the accuracy will be deteriorated when the diffusivity ε is getting small (see also [26]). In practice, the fourth-order compact difference approximations may be over-smoothed when the mesh-Péclet number is greater than one.

In this paper, we will devise a new finite difference scheme of accuracy $\mathcal{O}(\varepsilon^2(h+k) +$

$\varepsilon(h^2+k^2)+(h^3+k^3))$ for problem (1.1) with a small diffusivity ε. With a novel treatment for the reaction term, we first derive a difference scheme of accuracy $\mathcal{O}(\varepsilon^2 h+\varepsilon h^2+h^3)$ for the 1-D case. Employing the alternating direction technique [6, 24], we then extend the scheme to the 2-D case on a nine-point compact stencil with an accuracy of $\mathcal{O}(\varepsilon^2(h+k)+\varepsilon(h^2+k^2)+(h^3+k^3))$. Finally, as the basis of a discretization method for the 2-D incompressible Navier-Stokes equations, the high-accuracy difference scheme is applied to solve the steady incompressible viscous flow problem in the stream function-vorticity formulation for various Reynolds numbers. For the numerical verification, we provide a series of examples, including the lid-driven cavity flow problem, to illustrate the performance of the proposed scheme. The numerical results obtained are also compared with some higher-order difference schemes in the literature, such as the polynomial and exponential compact schemes [18–21, 24]. From these comparisons, we may observe that the newly proposed scheme can achieve good accuracy with a better stability when the diffusivity ε is small.

In [6], we have proposed an enhanced upwind difference scheme for solving the problem (1.1) with a constant convection field (i.e., a is a constant vector) but without the reaction term (i.e., $\sigma=0$), and then apply the enhanced scheme to solve a coupled system of convection-diffusion equations arising from the steady incompressible magnetohydrodynamic duct flow problem. In this paper, based on the work of [6], the newly proposed high-accuracy difference scheme is devised to solve the problem (1.1) with a variable convection field and a non-vanishing reaction term. Indeed, we propose a novel technique for treating the reaction term to obtain the desired high accuracy. We emphasize that it would be difficult to reach the desired high accuracy if a more direct approach is used instead of the specific treatment for the reaction term. This point will be demonstrated more clearly in Remark 2.1 in Section 2.

The remainder of this paper is organized as follows. We derive the high-accuracy difference scheme for 1-D problems with a small diffusivity in Section 2 and then extend the scheme to the 2-D case by using the alternating direction technique in Section 3. In Section 4, we apply the scheme to solve the 2-D steady incompressible Navier-Stokes equations in the stream function-vorticity formulation. In Section 5, numerical examples are presented to illustrate the effectiveness of the high-accuracy difference scheme. Finally, a summary and conclusions are given in Section 6.

2   The high-accuracy finite difference scheme: 1-D case

We first consider the following equation with a constant convection coefficient:

$$-\varepsilon u''(x)+au'(x)+\sigma u(x)=f(x) \quad \text{for } x\in(c_1,c_2), \tag{2.1}$$

where $0<\varepsilon\ll 1$, a and $\sigma\geq 0$ are both constant, and $f(x)$ is a given smooth function. Let x_i be an interior grid point of a uniform grid on (c_1,c_2) with grid size h and u_i the finite difference approximation to $u(x)$ at the grid point x_i. The second-order central difference

approximation to(2.1) at x_i is given by

$$-\varepsilon\delta_x^2 u_i + a\delta_x u_i + \sigma u_i = f_i \tag{2.2}$$

with a local truncation error term

$$\tau_i := \frac{ah^2}{6}u^{(3)}(x_i) - \frac{\varepsilon h^2}{12}u^{(4)}(x_i) + \mathcal{O}(h^4), \tag{2.3}$$

where $f_i := f(x_i)$ and the δ-operators are defined as

$$\delta_x^2 u_i := \frac{u_{i+1} - 2u_i + u_{i-1}}{h^2} \quad \text{and} \quad \delta_x u_i := \frac{u_{i+1} - u_{i-1}}{2h}. \tag{2.4}$$

It was already known that the central difference scheme (2.2) is unstable. When the diffusivity ε is small enough such that the mesh-Péclet number $Pe_h := |a|h/(2\varepsilon)$ is greater than one, large spurious oscillations may appear in the numerical solutions. On the other hand, applying the central difference rule to $u''(x_i)$ and the upwind difference rule to $au'(x_i)$, we obtain the stable upwind scheme of accuracy $\mathcal{O}(h)$,

$$-\left(\varepsilon + \frac{|a|h}{2}\right)\delta_x^2 u_i + a\delta_x u_i + \sigma u_i = f_i, \tag{2.5}$$

where the local truncation error term τ_i is given by

$$\tau_i := -\frac{ah}{2}u''(x_i) + \mathcal{O}(h^2). \tag{2.6}$$

The underlying idea behind the Spotz compact approach [20] is to find compact approximations to the derivatives in (2.3) by differentiating (2.1) at x_i,

$$u^{(3)}(x_i) = \frac{1}{\varepsilon}\left(au''(x_i) + \sigma u'(x_i) - f_i'\right), \tag{2.7a}$$

$$u^{(4)}(x_i) = \frac{1}{\varepsilon^2}\left((a^2 + \sigma\varepsilon)u''(x_i) + a\sigma u'(x_i) - af_i' - \varepsilon f_i''\right), \tag{2.7b}$$

where we use the notation $f_i' := f'(x_i)$ and $f_i'' := f''(x_i)$. Substituting (2.7a) and (2.7b) into (2.3) and applying the central difference rules to the derivatives therein yields

$$\tau_i = \frac{h^2}{12\varepsilon}\left((a^2 - \sigma\varepsilon)\delta_x^2 u(x_i) + a\sigma\delta_x u(x_i) - af_i' + \varepsilon f_i''\right) + \mathcal{O}(h^4/\varepsilon). \tag{2.8}$$

Thus, the resulting compact difference scheme of Spotz is given by

$$-\left(\varepsilon + \frac{(a^2 - \sigma\varepsilon)h^2}{12\varepsilon}\right)\delta_x^2 u_i + \left(a - \frac{a\sigma h^2}{12\varepsilon}\right)\delta_x u_i + \sigma u_i = f_i - \frac{ah^2}{12\varepsilon}f_i' + \frac{h^2}{12}f_i''. \tag{2.9}$$

Although the compact difference scheme (2.9) is of fourth-order of accuracy, one can observe from (2.8) that the accuracy of the scheme will be deteriorated when the diffusivity

ε is getting small. Moreover, the numerical solutions produced by (2.9) may be over-smoothed when the mesh-Péclet number is greater than one.

In our recent work [6], we have proposed the following scheme for (2.1) without the reaction term σu:

$$-\left(\varepsilon+\frac{|a|h}{2}\right)\delta_x^2 u_i+a\delta_x u_i=f_i+C_1 f_i'+C_2 f_i'', \tag{2.10}$$

where C_1 and C_2 are given by

$$C_1=-\frac{|a|h}{2a} \quad \text{and} \quad C_2=\frac{a^2h^2-3\varepsilon|a|h}{6a^2}. \tag{2.11}$$

This scheme reaches an accuracy of $\mathcal{O}(\varepsilon^2 h+\varepsilon h^2+h^3)$. We refer the reader to [6] for more details. Now we will generalize scheme (2.10) to solve (2.1) with a non-vanishing reaction term. We first rewrite (2.1) as

$$-\varepsilon u''(x)+au'(x)=F(x) \quad \text{for } x\in(c_1,c_2), \tag{2.12}$$

where F is defined by

$$F(x):=f(x)-\sigma u(x) \quad \text{for } x\in(c_1,c_2). \tag{2.13}$$

Notice that here we move the reaction term σu to the right-hand side in (2.12). This is a crucial step for obtaining the difference scheme with the desired accuracy. Applying scheme (2.10) to (2.12), we have

$$-\left(\varepsilon+\frac{|a|h}{2}\right)\delta_x^2 u_i+a\delta_x u_i=F_i+C_1 F_i'+C_2 F_i'' \tag{2.14}$$

with an accuracy of $\mathcal{O}(\varepsilon^2 h+\varepsilon h^2+h^3)$. Using the second-order central difference rules to approximate $u'(x_i)$ and $u''(x_i)$ involved in F_i' and F_i'', respectively, we obtain

$$-\left(\varepsilon+\frac{|a|h}{2}\right)\delta_x^2 u_i+a\delta_x u_i=f_i-\sigma u_i+C_1\left(f_i'-\sigma\delta_x u_i+\mathcal{O}(h^2)\right)$$
$$+C_2\left(f_i''-\sigma\delta_x^2 u_i+\mathcal{O}(h^2)\right). \tag{2.15}$$

Rearranging (2.15), we find the following finite difference scheme for (2.1),

$$-\left(\varepsilon+\frac{|a|h}{2}-\sigma C_2\right)\delta_x^2 u_i+\left(a+\sigma C_1\right)\delta_x u_i+\sigma u_i=f_i+C_1 f_i'+C_2 f_i'', \tag{2.16}$$

which still has an accuracy of $\mathcal{O}(\varepsilon^2 h+\varepsilon h^2+h^3)$.

We next consider the following 1-D reaction-convection-diffusion equation with a variable convection coefficient $a(x)$,

$$-\varepsilon u''(x)+a(x)u'(x)+\sigma u(x)=f(x) \quad \text{for } x\in(c_1,c_2). \tag{2.17}$$

Let $a_i := a(x_i)$. Applying scheme (2.16) to the following equation with a constant convection coefficient,

$$-\varepsilon u''(x) + a_i u'(x) + \sigma u(x) = f(x), \tag{2.18}$$

we have

$$-\left(\varepsilon + \frac{|a_i|h}{2} - \sigma C_2\right)\delta_x^2 u_i + \left(a_i + \sigma C_1\right)\delta_x u_i + \sigma u_i = f_i + C_1 f_i' + C_2 f_i'', \tag{2.19}$$

where C_1 and C_2 are given in (2.11), but a is replaced by a_i, namely,

$$C_1 := -\frac{|a_i|h}{2a_i} \quad \text{and} \quad C_2 := \frac{a_i^2 h^2 - 3\varepsilon |a_i| h}{6a_i^2}. \tag{2.20}$$

Based on the idea proposed in [16], we can study how accurate the scheme (2.19) approximates (2.17) at $x = x_i$ when we replace $\delta_x^2 u_i$, $\delta_x u_i$ and u_i by $\delta_x^2 u(x_i)$, $\delta_x u(x_i)$ and $u(x_i)$, respectively. Using the Taylor expansion, one can show that

$$-\varepsilon u''(x_i) + a(x_i)u'(x_i) + \sigma u(x_i) - C_1 a'(x_i)u'(x_i) - C_2\left(a''(x_i)u'(x_i) + 2a'(x_i)u''(x_i)\right)$$
$$= f(x_i) + \mathcal{O}(\varepsilon^2 h + \varepsilon h^2 + h^3). \tag{2.21}$$

From this observation, we may modify scheme (2.19) as

$$-\left(\varepsilon + \frac{|a_i|h}{2} - \sigma C_2 - 2a_i' C_2\right)\delta_x^2 u_i + \left(a_i + \sigma C_1 + a_i' C_1 + a_i'' C_2\right)\delta_x u_i + \sigma u_i$$
$$= f_i + C_1 f_i' + C_2 f_i'', \tag{2.22}$$

which is a finite difference scheme for approximating equation (2.17) with an accuracy of $\mathcal{O}(\varepsilon^2 h + \varepsilon h^2 + h^3)$. If $\sigma = 0$ then scheme (2.22) is changed into

$$-\left(\varepsilon + \frac{|a_i|h}{2} - 2a_i' C_2\right)\delta_x^2 u_i + \left(a_i + a_i' C_1 + a_i'' C_2\right)\delta_x u_i = f_i + C_1 f_i' + C_2 f_i''. \tag{2.23}$$

Remark 2.1. In the derivation of scheme (2.16), we first move the reaction term σu to the right-hand side as a part of the source term; see (2.12). Without this specific treatment for the reaction term, it would be difficult to reach the desired high accuracy of $\mathcal{O}(\varepsilon^2 h + \varepsilon h^2 + h^3)$. We now demonstrate this point in more details as follows. Assume that a is a constant and $\sigma \neq 0$. We are aiming to approximate (2.1) at the grid point x_i in the form

$$-\left(\varepsilon + \frac{|a|h}{2}\right)\delta_x^2 u(x_i) + a\delta_x u(x_i) + \sigma u(x_i) = C_0 f_i + C_1 f_i' + C_2 f_i'', \tag{2.24}$$

where C_0, C_1 and C_2 are coefficients needed to be determined such that the resulting difference scheme is consistent and with a truncation error as small as possible. Now, just as we did in [6], using the Taylor expansion we obtain

$$-\left(\varepsilon + \frac{|a|h}{2}\right)\left(u''(x_i) + \frac{h^2}{12}u^{(4)}(x_i) + \mathcal{O}(h^4)\right) + a\left(u'(x_i) + \frac{h^2}{6}u^{(3)}(x_i) + \mathcal{O}(h^4)\right) + \sigma u(x_i)$$
$$= C_0\left(-\varepsilon u''(x_i) + au'(x_i) + \sigma u(x_i)\right) + C_1\left(-\varepsilon u^{(3)}(x_i) + au''(x_i) + \sigma u'(x_i)\right)$$
$$+ C_2\left(-\varepsilon u^{(4)}(x_i) + au^{(3)}(x_i) + \sigma u''(x_i)\right). \tag{2.25}$$

Rearranging the above equation, we have

$$
\begin{aligned}
&-\varepsilon u''(x_i) + au'(x_i) + \sigma u(x_i) \\
&= f_i + (C_0\sigma - \sigma)u(x_i) + (C_0 a + C_1\sigma - a)u'(x_i) \\
&\quad + \Big(\varepsilon + \frac{|a|h}{2} - C_0\varepsilon + C_1 a + C_2\sigma\Big)u''(x_i) + \Big(C_2 a - C_1\varepsilon - \frac{ah^2}{6}\Big)u^{(3)}(x_i) \\
&\quad + \Big(\frac{\varepsilon h^2}{12} + \frac{|a|h^3}{24} - C_2\varepsilon\Big)u^{(4)}(x_i) + \mathcal{O}(\varepsilon h^4) + \mathcal{O}(h^4).
\end{aligned}
\tag{2.26}
$$

For the consistency of the resulting finite difference scheme, we may, for example, take

$$
C_0\sigma - \sigma = 0, \quad C_0 a + C_1\sigma - a = 0 \quad \text{and} \quad \varepsilon + \frac{|a|h}{2} - C_0\varepsilon + C_1 a + C_2\sigma = 0,
\tag{2.27}
$$

i.e.,

$$
C_0 = 1, \quad C_1 = 0 \quad \text{and} \quad C_2 = -|a|h/(2\sigma),
\tag{2.28}
$$

and then the truncation error becomes

$$
\Big(C_2 a - C_1\varepsilon - \frac{ah^2}{6}\Big)u^{(3)}(x_i) + \Big(\frac{\varepsilon h^2}{12} + \frac{|a|h^3}{24} - C_2\varepsilon\Big)u^{(4)}(x_i) + \mathcal{O}(\varepsilon h^4) + \mathcal{O}(h^4) = \mathcal{O}(h).
$$

In other words, the difference scheme (2.24) with coefficients (2.28) is $\mathcal{O}(h)$ accurate, which does not reach the desired high accuracy of $\mathcal{O}(\varepsilon^2 h + \varepsilon h^2 + h^3)$.

3   The high-accuracy finite difference scheme: 2-D case

In this section, using the technique of alternating direction (cf. [6, 24]), we will extend the high-accuracy finite difference scheme (2.22) to adapt to the 2-D problem (1.1) with a small diffusivity ε. To simplify the presentation, we assume that the 2-D domain Ω is a rectangular region given by $\Omega = (c_1, c_2) \times (d_1, d_2)$. Let $x_i = c_1 + ih$ and $y_j = d_1 + jk$ for $i = 0, 1, \cdots, m$ and $j = 0, 1, \cdots, n$, where $h := (c_2 - c_1)/m$ and $k := (d_2 - d_1)/n$ denote the grid sizes in the x- and y-directions, respectively. We denote by $u_{i,j}$ the approximation to $u(x, y)$ at the grid point (x_i, y_j). The δ-operators, δ_x, δ_y, δ_x^2 and δ_y^2, acting on $u(x_i, y_j)$ and $u_{i,j}$ are defined in a usual way (cf. (2.4)).

From the 2-D differential equation in (1.1), we have

$$
-\varepsilon u_{xx}(x, y) + a_1(x, y)u_x(x, y) = F_1(x, y) \quad \text{for } (x, y) \in \Omega,
\tag{3.1a}
$$
$$
-\varepsilon u_{yy}(x, y) + a_2(x, y)u_y(x, y) = F_2(x, y) \quad \text{for } (x, y) \in \Omega,
\tag{3.1b}
$$

where the functions F_1 and F_2 are given by

$$
F_1(x, y) := f(x, y) - \big(-\varepsilon u_{yy}(x, y) + a_2(x, y)u_y(x, y) + \sigma u(x, y)\big),
\tag{3.2a}
$$
$$
F_2(x, y) := f(x, y) - \big(-\varepsilon u_{xx}(x, y) + a_1(x, y)u_x(x, y) + \sigma u(x, y)\big).
\tag{3.2b}
$$

Notice that the sum of (3.1a) and (3.1b) gives the original equation in (1.1). As usual, we define $a_{1i,j} := a_1(x_i, y_j)$ and $a_{2i,j} := a_2(x_i, y_j)$. Next, we are going to approximate (3.1a) and (3.1b) at the grid point (x_i, y_j). To discretize (3.1a) at (x_i, y_j), we apply the 1-D high-accuracy difference scheme (2.23) (i.e., (2.22) with $\sigma = 0$) if $|a_{1i,j}| h / (2\varepsilon) > 1$; otherwise, if $|a_{1i,j}| h / (2\varepsilon) \leq 1$, we employ the Spotz fourth-order compact scheme (2.9) with $\sigma = 0$. A similar strategy is applied to discretize (3.1b) as well. In what follows, we assume that $|a_{1ij}| h / (2\varepsilon) > 1$ and $|a_{2ij}| k / (2\varepsilon) > 1$ to simplify the presentation.

Applying the 1-D high-accuracy difference scheme (2.23) to discretize (3.1a) and (3.1b) at (x_i, y_j), we obtain

$$
-\left(\varepsilon + \frac{|a_1| h}{2} - 2a_{1x}\alpha_2\right)_{i,j} \delta_x^2 u_{i,j} + \left(a_1 + a_{1x}\alpha_1 + a_{1xx}\alpha_2\right)_{i,j} \delta_x u_{i,j}
$$
$$
= \left(F_1 + \alpha_1 F_{1x} + \alpha_2 F_{1xx}\right)_{i,j}, \tag{3.3a}
$$
$$
-\left(\varepsilon + \frac{|a_2| k}{2} - 2a_{2y}\beta_2\right)_{i,j} \delta_y^2 u_{i,j} + \left(a_2 + a_{2y}\beta_1 + a_{2yy}\beta_2\right)_{i,j} \delta_y u_{i,j}
$$
$$
= \left(F_2 + \beta_1 F_{2y} + \beta_2 F_{2yy}\right)_{i,j}, \tag{3.3b}
$$

where the notation $(G)_{i,j}$ denotes $G(x_i, y_j)$ for a given function G and

$$
\alpha_1 := -\left(\frac{|a_1| h}{2a_1}\right)_{i,j}, \qquad \alpha_2 := \left(\frac{a_1^2 h^2 - 3\varepsilon |a_1| h}{6a_1^2}\right)_{i,j}, \tag{3.4a}
$$
$$
\beta_1 := -\left(\frac{|a_2| k}{2a_2}\right)_{i,j}, \qquad \beta_2 := \left(\frac{a_2^2 k^2 - 3\varepsilon |a_2| k}{6a_2^2}\right)_{i,j}. \tag{3.4b}
$$

Next taking the sum of (3.3a) and (3.3b), we obtain a difference scheme for (1.1) with accuracy of $\mathcal{O}(\varepsilon^2(h+k) + \varepsilon(h^2+k^2) + (h^3+k^3))$:

$$
-\left(\varepsilon + \frac{|a_1| h}{2} - 2a_{1x}\alpha_2\right)_{i,j} \delta_x^2 u_{i,j} - \left(\varepsilon + \frac{|a_2| k}{2} - 2a_{2y}\beta_2\right)_{i,j} \delta_y^2 u_{i,j}
$$
$$
+ \left(a_1 + a_{1x}\alpha_1 + a_{1xx}\alpha_2\right)_{i,j} \delta_x u_{i,j} + \left(a_2 + a_{2y}\beta_1 + a_{2yy}\beta_2\right)_{i,j} \delta_y u_{i,j}
$$
$$
= \left(F_1 + F_2 + \alpha_1(F_{1x} + F_{2x}) + \alpha_2(F_{1xx} + F_{2xx}) + \beta_1(F_{1y} + F_{2y}) + \beta_2(F_{1yy} + F_{2yy})\right.
$$
$$
\left. - \alpha_1 F_{2x} - \alpha_2 F_{2xx} - \beta_1 F_{1y} - \beta_2 F_{1yy}\right)_{i,j}. \tag{3.5}
$$

Using the identity $f - \sigma u = F_1 + F_2$, the right-hand side of (3.5) can be simplified as

$$
\left(f + \alpha_1 f_x + \alpha_2 f_{xx} + \beta_1 f_y + \beta_2 f_{yy} - \sigma u - (\alpha_1 \sigma + \beta_1 a_{1y} + \beta_2 a_{1yy})u_x - \alpha_2 \sigma u_{xx}\right.
$$
$$
- (\beta_1 \sigma + \alpha_1 a_{2x} + \alpha_2 a_{2xx})u_y - \beta_2 \sigma u_{yy} - (\alpha_1 a_2 + 2\alpha_2 a_{2x} + \beta_1 a_1 + 2\beta_2 a_{1y})u_{xy}
$$
$$
\left. + (\beta_1 \varepsilon - \alpha_2 a_2)u_{xxy} + (\alpha_1 \varepsilon - \beta_2 a_1)u_{xyy} + (\alpha_2 \varepsilon + \beta_2 \varepsilon)u_{xxyy}\right)_{i,j}. \tag{3.6}
$$

We then use the following standard second-order finite difference rules to approximate the derivative terms u_x, u_{xx}, u_y, u_{yy}, u_{xy}, u_{xxy}, u_{xyy}, and u_{xxyy} at (x_i, y_j) in (3.6):

$$(u_x)_{i,j} = \delta_x u(x_i, y_j) + \mathcal{O}(h^2), \qquad (u_y)_{i,j} = \delta_y u(x_i, y_j) + \mathcal{O}(k^2),$$
$$(u_{xx})_{i,j} = \delta_x^2 u(x_i, y_j) + \mathcal{O}(h^2), \qquad (u_{yy})_{i,j} = \delta_y^2 u(x_i, y_j) + \mathcal{O}(k^2),$$
$$(u_{xy})_{i,j} = \delta_y \delta_x u(x_i, y_j) + \mathcal{O}(h^2 + k^2), \qquad (u_{xxy})_{i,j} = \delta_y \delta_x^2 u(x_i, y_j) + \mathcal{O}(h^2 + k^2),$$
$$(u_{xyy})_{i,j} = \delta_y^2 \delta_x u(x_i, y_j) + \mathcal{O}(h^2 + k^2), \qquad (u_{xxyy})_{i,j} = \delta_y^2 \delta_x^2 u(x_i, y_j) + \mathcal{O}(h^2 + k^2).$$

Finally, by neglecting the high-order error terms in the resulting equation, we obtain the desired difference scheme of accuracy $\mathcal{O}(\varepsilon^2(h+k) + \varepsilon(h^2+k^2) + (h^3+k^3))$ for the 2-D reaction-convection-diffusion problem (1.1) with a small ε:

$$
\begin{aligned}
&- \left(\varepsilon + \frac{|a_1|h}{2} - 2a_{1x}\alpha_2 - \alpha_2\sigma \right)_{i,j} \delta_x^2 u_{i,j} - \left(\varepsilon + \frac{|a_2|k}{2} - 2a_{2y}\beta_2 - \beta_2\sigma \right)_{i,j} \delta_y^2 u_{i,j} \\
&+ \left(a_1 + a_{1x}\alpha_1 + a_{1xx}\alpha_2 + \alpha_1\sigma + \beta_1 a_{1y} + \beta_2 a_{1yy} \right)_{i,j} \delta_x u_{i,j} \\
&+ \left(a_2 + a_{2y}\beta_1 + a_{2yy}\beta_2 + \beta_1\sigma + \alpha_1 a_{2x} + \alpha_2 a_{2xx} \right)_{i,j} \delta_y u_{i,j} \\
&+ \left(\alpha_1 a_2 + 2\alpha_2 a_{2x} + \beta_1 a_1 + 2\beta_2 a_{1y} \right)_{i,j} \delta_y \delta_x u_{i,j} + \left(\alpha_2 a_2 - \beta_1 \varepsilon \right)_{i,j} \delta_y \delta_x^2 u_{i,j} \\
&+ \left(\beta_2 a_1 - \alpha_1 \varepsilon \right)_{i,j} \delta_y^2 \delta_x u_{i,j} - \left(\alpha_2 \varepsilon + \beta_2 \varepsilon \right) \delta_y^2 \delta_x^2 u_{i,j} + \sigma u_{i,j} \\
&= \left(f + \alpha_1 f_x + \alpha_2 f_{xx} + \beta_1 f_y + \beta_2 f_{yy} \right)_{i,j}.
\end{aligned}
\tag{3.7}
$$

We remark that if $|a_{1ij}|h/(2\varepsilon) \le 1$ or $|a_{2ij}|k/(2\varepsilon) \le 1$ then a high-accuracy difference scheme can be derived in a similar way. For example, assume that $|a_{1ij}|h/(2\varepsilon) \le 1$ and $|a_{2ij}|k/(2\varepsilon) > 1$. Then, in this case, we use the Spotz fourth-order compact difference scheme (2.9) with $\sigma = 0$ to approximate (3.1a), while the 1-D high-accuracy difference scheme (2.23) to discretize (3.1b). However, for the sake of simplicity, we still call the resulting scheme *"high-accuracy difference scheme (3.7)"*.

4   Application to the incompressible Navier-Stokes equations

In this section, the newly proposed high-accuracy difference scheme (3.7) is used as the basis of a discretization method for the 2-D steady incompressible Navier-Stokes equations in the stream function-vorticity formulation. The system of equations in the primitive variables formulation is given by

$$
\begin{aligned}
-\nu\Delta u + (u \cdot \nabla)u + \nabla p &= f &&\text{in } \Omega, &&(4.1a) \\
\nabla \cdot u &= 0 &&\text{in } \Omega, &&(4.1b)
\end{aligned}
$$

where $u = (u,v)^\top$ is the velocity field, p is the pressure, ν is the kinematic viscosity, and $f = (f_1, f_2)^\top$ is a given forcing term. Introducing the vorticity ω,

$$\omega := \nabla \times u = v_x - u_y \quad \text{in } \Omega, \tag{4.2}$$

and applying the curl operator to (4.1a), the pressure gradient term disappears and

$$-\nu\Delta\omega+\boldsymbol{u}\cdot\nabla\omega=f_{2x}-f_{1y}\quad\text{in }\Omega.\tag{4.3}$$

The velocity field $\boldsymbol{u}=(u,v)^\top$ is defined in terms of the stream function ψ by

$$\boldsymbol{u}=\nabla\times\psi:=(\psi_y,-\psi_x)^\top\quad\text{in }\Omega.\tag{4.4}$$

The equation satisfied by ψ is obtained by applying the curl operator to (4.4),

$$-\Delta\psi-\omega=0\quad\text{in }\Omega.\tag{4.5}$$

The system of Eqs. (4.3)-(4.5) is the so-called stream function-vorticity formulation of the 2-D steady incompressible Navier-Stokes equations.

The system of Eqs. (4.3)-(4.5) should be supplemented with some suitable boundary conditions. We consider the no-slip, no-penetration boundary conditions on $\partial\Omega$ as follows [21]:

$$\frac{\partial\psi}{\partial\boldsymbol{n}}=V\qquad\text{on }\partial\Omega,\tag{4.6a}$$

$$\frac{\partial\psi}{\partial\boldsymbol{t}}=0\qquad\text{on }\partial\Omega,\tag{4.6b}$$

where $\boldsymbol{n}$ is the outward unit vector normal to $\partial\Omega$, $\boldsymbol{t}$ is the unit vector tangent to $\partial\Omega$ with clockwise orientation, and V is the tangential wall velocity. The latter equation (4.6b) implies ψ is constant on $\partial\Omega$. For simplicity, it will be set equal to zero on $\partial\Omega$.

Note that the boundary conditions (4.6a) and (4.6b) do not involve the vorticity ω. Therefore, if we attempt to solve the vorticity equation (4.3) alone (e.g., as part of a block-iterative algorithm applied to the fully coupled system), the system will be underspecified because there is no immediate way to obtain vorticity values on $\partial\Omega$. However, suitable boundary conditions for the vorticity ω can be obtained from the discretization of (4.6a) by using the fourth-order Jensen's formulation on the $\partial\Omega$. We refer the reader to [21]. The reader is also referred to [4, 5, 11, 20, 22, 24] and many references cited therein for some higher-order difference discretizations of the 2-D steady incompressible Navier-Stokes equations.

To summarize, the proposed high-accuracy difference scheme (3.7) is applied to solve the vorticity equation (4.3), while the Poisson equation (4.5) is solved by Spotz's fourth-order compact difference scheme [20]. In Section 5, we perform numerical experiments of the lid-driven cavity flow problem with various Reynolds numbers.

5   Numerical experiments

In this section, a number of examples is presented to illustrate the high performance of the newly proposed difference scheme (3.7). We will consider examples exhibiting

boundary or interior layers, including the lid-driven cavity flow problem. The numerical results obtained are compared with those of some high-order compact difference schemes in the literature, including the schemes of Spotz [20, 21], Tian-Dai [24] and Sanyasiraju-Mishra [18, 19]. We remark that using the similar technique as in Section 2 for treating the reaction term σu, the Tian-Dai scheme can be easily extended to solve problems with a non-vanishing reaction term. However, it seems not easy to do so for the Sanyasiraju-Mishra scheme. From the comparisons, we may observe that for a small diffusivity ε, our scheme (3.7) can achieve good accuracy with a better stability.

In order to simplify the numerical implementation, we partition the domain Ω into a uniform grid in all testings. In the first two examples, in which the exact solution is known, we can calculate the errors of numerical solutions and then estimate the convergence rates. For measuring the global errors of the finite difference approximations, we use the usual max-norm and discrete L^2-norm (cf. [10]).

Example 5.1 (An interior layer problem with an analytic solution). This example is taken from [18] with a slight modification. We consider the Dirichlet boundary value problem for the differential equation

$$-\varepsilon\Delta u+(1,1)^{\top}\cdot\nabla u+u=f \quad \text{in } \Omega:=(0,1)\times(0,1)$$

with the exact solution $u(x,y)=e^{-(x^6+y^6)/\varepsilon}$, in which an interior layer appears approaching the left down corner when the diffusivity ε is getting small (cf. Fig. 1).

The numerical results for $\varepsilon = 10^{-\ell}$, $\ell = 2,3,4$, and different grid sizes, $h = 1/20,1/40,1/80,1/160$, are reported in Table 1 and Table 2, from which we have the findings that when the diffusivity ε is not too small, $\varepsilon = 10^{-2}$, all these difference schemes display a high-accuracy behavior. However, the high accuracy is deteriorated when the diffusivity ε is getting smaller. As $\varepsilon = 10^{-3}$ and $\varepsilon = 10^{-4}$, the Spotz scheme shows a lower accuracy than the others. We depict the contour plots of exact and numerical solutions for $\varepsilon = 10^{-\ell}$, $\ell = 2,3,4$ and $h = 1/40$ in Fig. 1.

Example 5.2 (A boundary layer problem with an analytic solution). This example is quoted from [24] with an additional reaction term. We consider the differential equation

$$-\varepsilon\Delta u+(0,1/(1+y))^{\top}\cdot\nabla u+3u=f \quad \text{in } \Omega:=(0,1)\times(0,1)$$

with the Dirichlet boundary condition, where the source function f is determined such that the exact solution is given by $u(x,y)=e^{y-x}+2^{-1/\varepsilon}(1+y)^{1+1/\varepsilon}$. When the diffusivity ε is small enough, a strong boundary layer appears near the up-edge of the boundary $\partial\Omega$; see the plot of exact solution given in Fig. 2 for $\varepsilon = 10^{-6}$.

The computed results of various difference schemes for different grid sizes are collected in Table 3 and Table 4. From the numerical results, we have the following observations. When the diffusivity ε is not too small, $\varepsilon = 10^{-2}$, all these difference schemes show a high-order accuracy. Again, the high accuracy is deteriorated when the diffusivity ε is getting smaller. In particular, as $\varepsilon \to 0^+$, the Spotz scheme tends to lose its accuracy. The

Table 1: Errors in the max-norm of the numerical solutions of Example 5.1.

ε	$1/h$	Spotz [20]		Tian-Dai [24]		Present scheme	
		Max-norm	Rate	Max-norm	Rate	Max-norm	Rate
10^{-2}	20	4.9627e-03	—	4.0555e-03	—	5.5884e-03	—
	40	3.5394e-04	3.81	3.4234e-04	3.57	1.0042e-03	2.48
	80	2.2260e-05	3.99	2.3060e-05	3.89	2.2260e-05	5.50
	160	1.3900e-06	4.00	1.4686e-06	3.97	1.3900e-06	4.00
10^{-3}	20	4.4128e-02	—	2.0136e-02	—	2.0528e-02	—
	40	8.8973e-03	2.31	3.0443e-03	2.73	3.2745e-03	2.65
	80	8.2670e-04	3.43	3.6288e-04	3.07	4.2502e-04	2.95
	160	5.4141e-05	3.93	3.7545e-05	3.27	5.2215e-05	3.02
10^{-4}	20	8.4587e-02	—	4.2045e-02	—	4.1993e-02	—
	40	3.6256e-02	1.22	9.2731e-03	2.18	9.3184e-03	2.17
	80	1.0540e-02	1.78	1.3465e-03	2.78	1.3664e-03	2.77
	160	1.5087e-03	2.80	1.6879e-04	3.00	1.7418e-04	2.97

Table 2: Errors in the discrete L^2-norm of the numerical solutions of Example 5.1.

ε	$1/h$	Spotz [20]		Tian-Dai [24]		Present scheme	
		Discrete L^2	Rate	Discrete L^2	Rate	Discrete L^2	Rate
10^{-2}	20	1.1323e-03	—	8.4543e-04	—	1.3359e-03	—
	40	7.8151e-05	3.86	6.7004e-05	3.66	2.9481e-04	2.18
	80	4.9121e-06	3.99	4.4835e-06	3.90	4.9121e-06	5.91
	160	3.9052e-07	3.65	3.8212e-07	3.55	3.9052e-07	3.65
10^{-3}	20	6.8732e-03	—	3.1500e-03	—	3.2078e-03	—
	40	1.4205e-03	2.27	5.3453e-04	2.56	5.7247e-04	2.49
	80	1.5664e-04	3.18	6.6171e-05	3.01	7.8495e-05	2.87
	160	1.0512e-05	3.90	6.7835e-06	3.29	1.0075e-05	2.96
10^{-4}	20	1.3235e-02	—	8.1021e-03	—	8.1061e-03	—
	40	4.0135e-03	1.72	1.2239e-03	2.73	1.2293e-03	2.72
	80	1.2867e-03	1.64	2.1626e-04	2.50	2.1933e-04	2.49
	160	2.2603e-04	2.51	2.9021e-05	2.90	2.9955e-05	2.87

overall accuracy of the numerical results produced by the Tian-Dai scheme seems better than the others. For $\varepsilon = 10^{-4}$, the proposed difference scheme (3.7) shows a rather poor convergence rate. With a closer inspection, we can find that the grid point at which the maximum error occurs is approaching to the up-left corner of the boundary layer as halving the grid size, see Table 5. However, for such a grid point being fixed, the errors in the max-norm approach to zero as $h \to 0^+$. Numerical results produced by various difference schemes for $\varepsilon = 10^{-6}$ with $h = 1/40$ are depicted in Fig. 2.

Example 5.3 (A boundary and interior layer problem)**.** This example is frequently used in the literature of finite element methods [7]. We consider the propagation of a discontinuity in the boundary data with a constant convection field $\boldsymbol{a}(x,y) = (1/2, \sqrt{3}/2)^\top$ of size
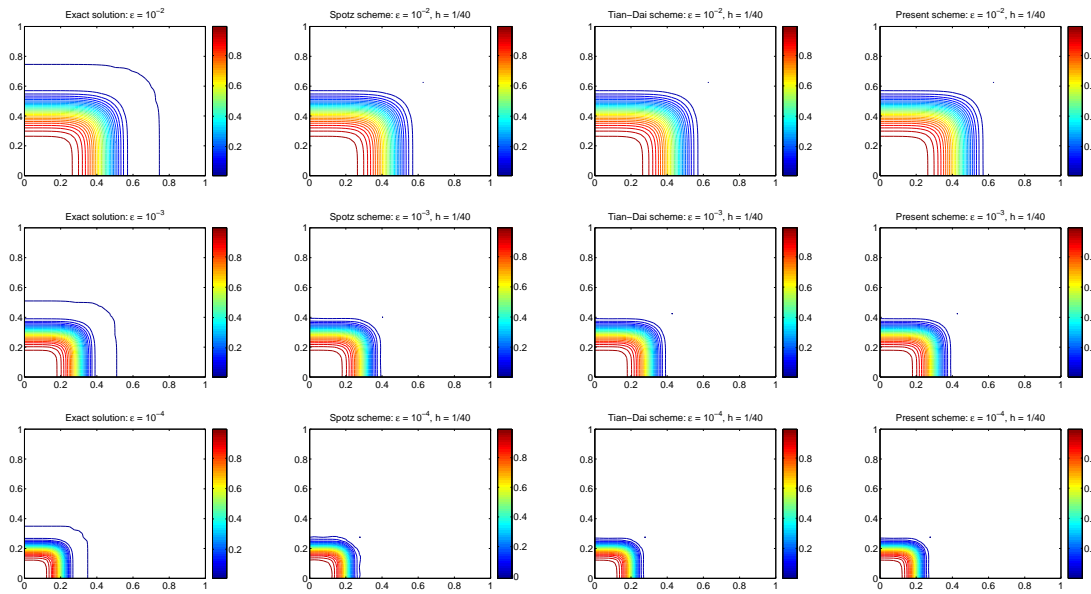
Figure 1: The contour plots of exact and numerical solutions of Example 5.1 with $\varepsilon = 10^{-\ell}$, $\ell = 2, 3, 4$, and $h = 1/40$.
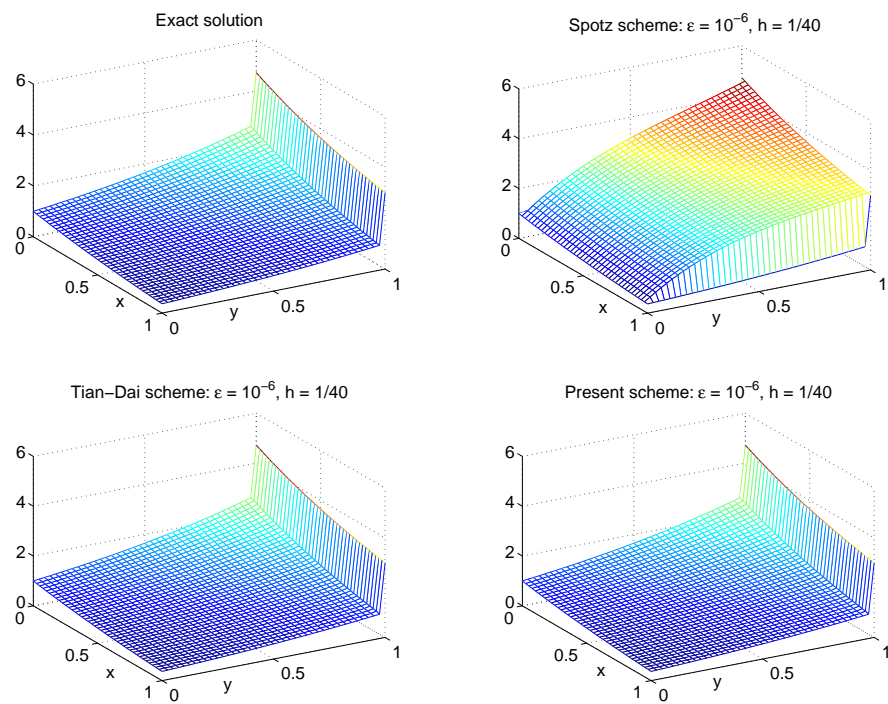

Figure 2: The elevation plots of exact and numerical solutions of Example 5.2 with $\varepsilon = 10^{-6}$ and $h = 1/40$.

Table 3: Errors in the max-norm of the numerical solutions of Example 5.2.

ε	$1/h$	Spotz [20]		Tian-Dai [24]		Present scheme	
		Max-norm	Rate	Max-norm	Rate	Max-norm	Rate
10^{-2}	20	4.2660e-02	—	1.2818e-02	—	3.6532e-01	—
	40	3.8070e-03	3.49	1.3905e-03	3.20	3.8070e-03	6.58
	80	2.2152e-04	4.10	8.5413e-05	4.02	2.2152e-04	4.10
	160	1.4146e-05	3.97	5.5432e-06	3.95	1.4146e-05	3.97
10^{-4}	20	1.9040e+00	—	4.2725e-02	—	5.3902e-02	—
	40	1.8182e+00	0.07	2.3420e-02	0.87	4.1053e-02	0.39
	80	1.6532e+00	0.14	1.2217e-02	0.94	4.4930e-02	-0.13
	160	1.3661e+00	0.28	6.1416e-03	0.99	6.9154e-02	-0.62
10^{-6}	20	1.9915e+00	—	4.2896e-02	—	4.6655e-02	—
	40	1.9946e+00	0.00	2.3594e-02	0.86	2.5750e-02	0.86
	80	1.9946e+00	0.00	1.2404e-02	0.93	1.3772e-02	0.90
	160	1.9918e+00	0.00	6.3637e-03	0.96	7.5558e-03	0.87

Table 4: Errors in the discrete L^2-norm of the numerical solutions of Example 5.2.

ε	$1/h$	Spotz [20]		Tian-Dai [24]		Present scheme	
		Discrete L^2	Rate	Discrete L^2	Rate	Discrete L^2	Rate
10^{-2}	20	9.2608e-03	—	2.7735e-03	—	8.2939e-02	—
	40	6.7264e-04	3.78	2.4488e-04	3.50	6.7264e-04	6.95
	80	4.1480e-05	4.02	1.5976e-05	3.94	4.1480e-05	4.02
	160	2.5578e-06	4.02	9.9950e-07	4.00	2.5578e-06	4.02
10^{-4}	20	1.1706e+00	—	8.9404e-03	—	1.1260e-02	—
	40	7.0140e-01	0.74	3.5190e-03	1.35	6.1615e-03	0.87
	80	3.2862e-01	1.09	1.3129e-03	1.42	4.8283e-03	0.35
	160	1.4726e-01	1.16	4.7323e-04	1.47	5.3367e-03	-0.14
10^{-6}	20	1.5060e+00	—	8.9578e-03	—	9.7233e-03	—
	40	1.5285e+00	-0.02	3.5284e-03	1.34	3.8442e-03	1.34
	80	1.4985e+00	0.03	1.3195e-03	1.42	1.4634e-03	1.39
	160	1.3376e+00	0.16	4.8002e-04	1.46	5.6962e-04	1.36

Table 5: The grid point (x_i, y_j) at which the maximum error occurs of the present difference scheme for $\varepsilon = 10^{-4}$ and different grid sizes, Example 5.2.

(x_i, y_j)	(0.05,0.95)	(0.025,0.975)	(0.0125,0.9875)	(0.00625,0.99375)
$1/h = 20$	5.3902e-02			
$1/h = 40$	6.1797e-04	4.1053e-02		
$1/h = 80$	1.7146e-07	8.0529e-04	4.4930e-02	
$1/h = 160$	4.1287e-08	2.4509e-06	2.1780e-03	6.9154e-02

one forming a 60° angle with the x-axis. In this test, we have

$$-\varepsilon \Delta u + \boldsymbol{a} \cdot \nabla u = 0 \quad \text{in } \Omega := (0,1) \times (0,1)$$

with the boundary conditions given by

$$\begin{cases} u=1 \text{ on } \{(x,y):x=0,\ 0\le y<1\}\cup\{(x,y):0\le x\le 1/2,\ y=0\}, \\ u=0 \text{ on } \{(x,y):0\le x\le 1,\ y=1\}\cup\{(x,y):x=1,\ 0\le y\le 1\} \\ \qquad \cup\{(x,y):1/2<x\le 1,\ y=0\}. \end{cases}$$

We consider the case of $\varepsilon=10^{-4}$. The elevation and contour plots of the numerical solutions of $h=1/32$ are displayed in Fig. 3, from which we find that the solution produced by the Spotz scheme [20] is almost collapsed (cf. Fig. 3 top), even if we use a relatively fine grid spacing. The other difference schemes are much better able to capture the interior and boundary layer structures in the solution, except some oscillation appearing near the interior layer region.

Example 5.4 (The double-glazing problem). This example is taken from [2]. Consider the following boundary value problem:

$$\begin{cases} -\varepsilon\Delta u+\boldsymbol{a}\cdot\nabla u=0 & \text{in } \Omega:=(-1,1)\times(-1,1), \\ u=0 & \text{on } \{(x,y):-1\le x<1,y=\pm 1\}\cup\{(x,y):x=-1,-1\le y\le 1\}, \\ u=1 & \text{on } \{(x,y):x=1,-1\le y\le 1\}. \end{cases}$$

This is a simple model for the temperature distribution in a cavity with an external wall that is "hot", where the convection field is given by

$$\boldsymbol{a}(x,y)=(2y(1-x^2),-2x(1-y^2))^\top,$$

which determines a recirculating flow. There are two discontinuities at the two corners of the hot wall and these discontinuities lead to boundary layers near these corners provided the diffusivity ε is small enough. When ε is getting smaller, boundary layers appear around the whole boundary $\partial\Omega$ of the domain, as shown in Fig. 5 below.

We consider the case of $\varepsilon=10^{-4}$. From the numerical results shown in Fig. 4 and Fig. 5, we can observe that all the Spotz, the Tian-Dai and the Sanyasiraju-Mishra schemes with $h=1/32$ lose their stability due to the large condition number of the resulting linear systems; see Table 6. However, reasonable results can be obtained if we take a finer grid size such as $h=1/128$ (cf. Fig. 5). The present difference scheme (3.7) always shows a reasonable accuracy with a better stability.

Table 6: The estimates of condition number of various difference schemes for $\varepsilon=10^{-4}$, Example 5.4.

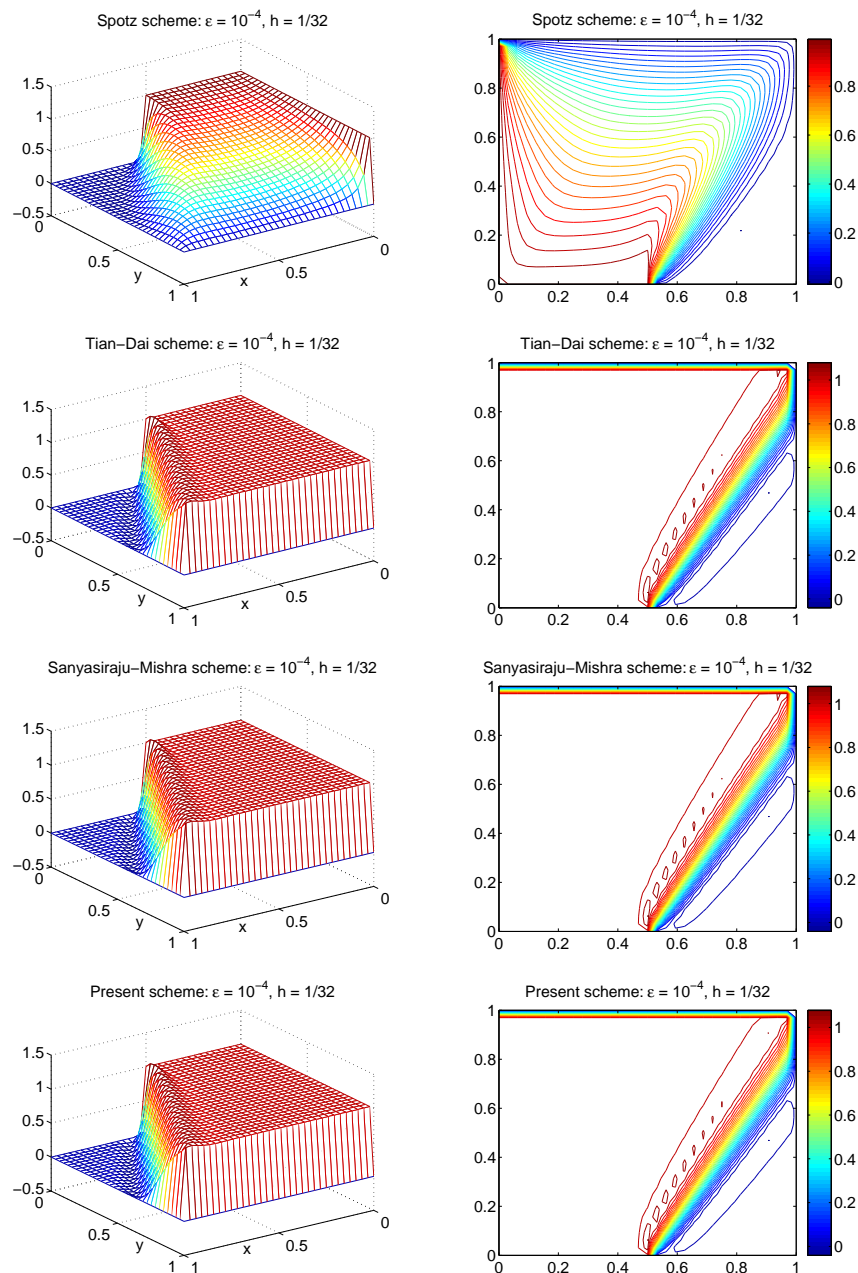|	$h=1/32$	$h=1/64$	$h=1/128$
Spotz [20]	2.0199e+09	5.1659e+07	3.9555e+07
Tian-Dai [24]	3.6284e+20	2.3641e+26	1.6593e+06
Sanyasiraju-Mishra [19]	1.2174e+21	1.3555e+25	1.6593e+06
Present scheme	5.3648e+05	9.4672e+05	1.8951e+06

Figure 3: The elevation and contour plots of numerical solutions of Example 5.3 with $\varepsilon=10^{-4}$ and $h=1/32$.

Example 5.5 (A nonlinear boundary layer problem). This example is quoted from [19]. We study the Dirichlet boundary value problem for the 2-D nonlinear equation

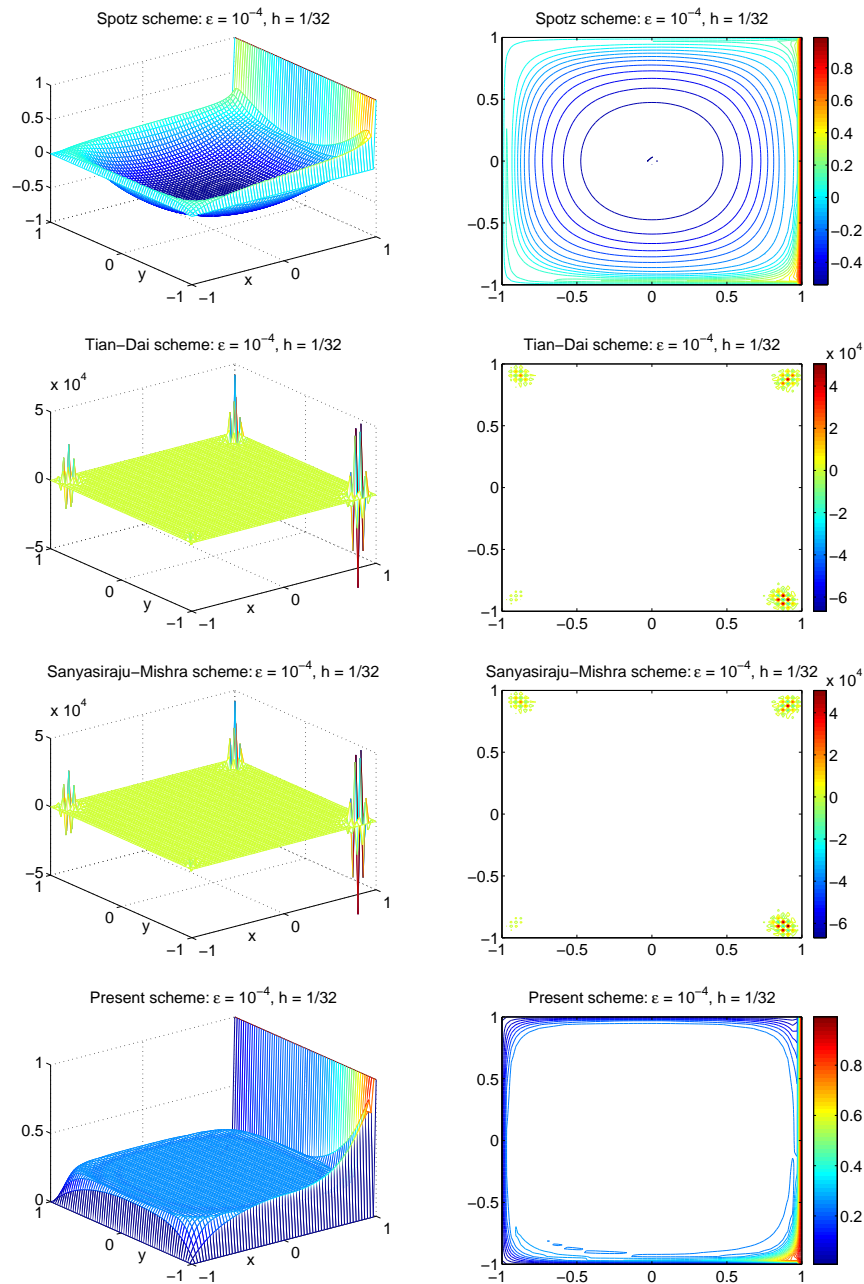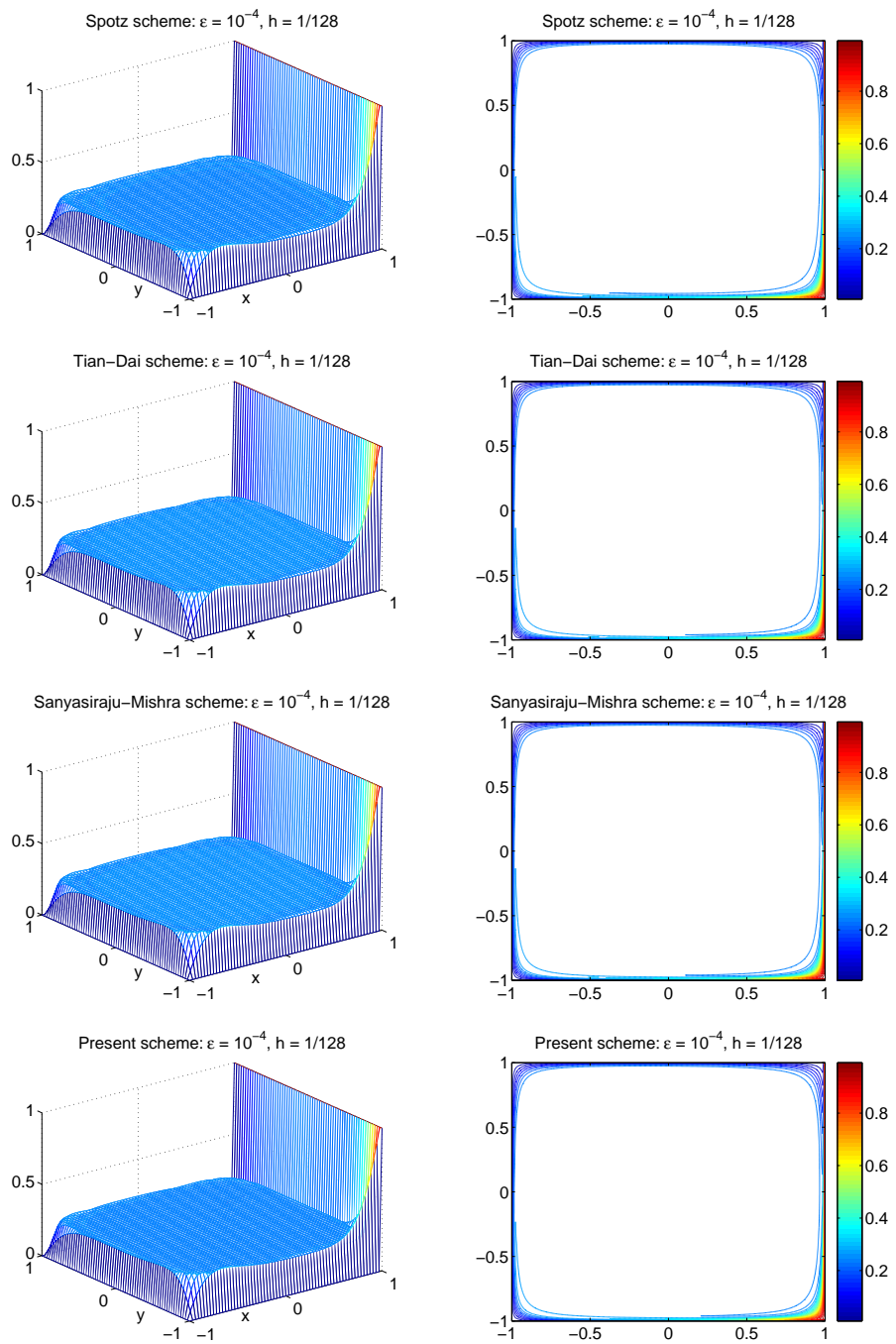$$-\varepsilon\Delta u + u u_x = f \quad \text{in } \Omega := (0,1)\times(0,1)$$

Figure 4: The elevation and contour plots of numerical solutions of Example 5.4 with $\varepsilon = 10^{-4}$ and $h = 1/32$.

with the exact solution $u(x,y) = \ln(1 + x/\varepsilon) + e^y$. When the diffusivity ε is small enough, a strong boundary layer appears near the left edge of the unit square domain Ω; see the plot of exact solution given in Fig. 6 for $\varepsilon = 10^{-2}$.

Figure 5: The elevation and contour plots of numerical solutions of Example 5.4 with $\varepsilon = 10^{-4}$ and $h = 1/128$.

For solving this nonlinear problem, an iterative successive over-relaxation procedure is associated with the present difference scheme (3.7). The grid values of partial deriva-
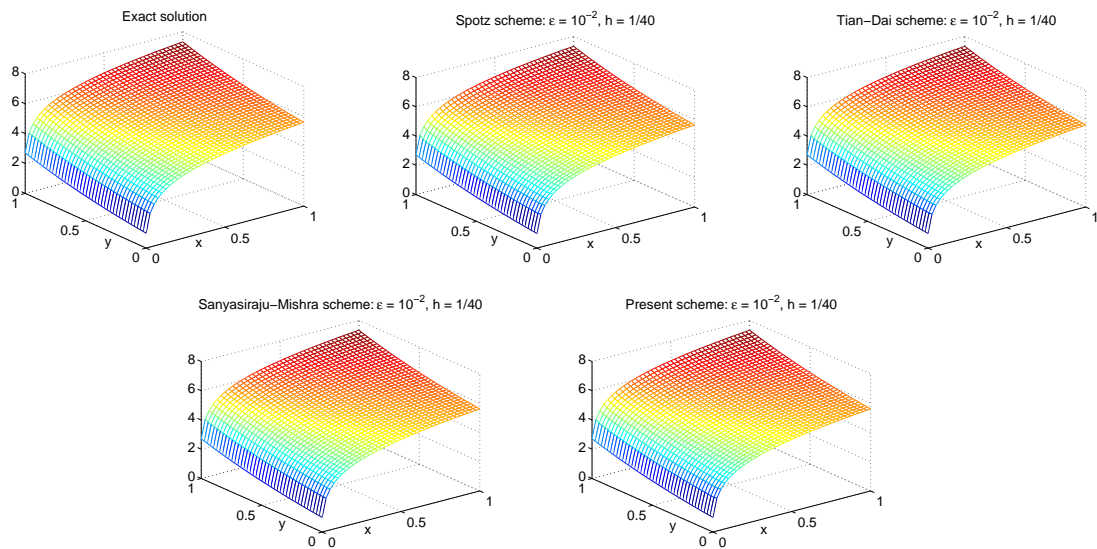
Figure 6: The elevation plots of exact and numerical solutions of Example 5.5 with $\varepsilon = 10^{-2}$ and $h = 1/40$.

tives of the convection coefficient required in the scheme (3.7) are computed at the beginning of the every iteration using the following fourth-order Padé scheme [13]

$$v'_{i-1} + 4v'_i + v'_{i+1} = \frac{3}{h}(v_{i+1} - v_{i-1}), \tag{5.1a}$$

$$v''_{i-1} + 10v''_i + v''_{i+1} = \frac{12}{h^2}(v_{i+1} - 2v_i + v_{i-1}), \tag{5.1b}$$

for $i = 1, 2, \cdots, m-1$, with third-order boundary closures

$$v'_0 + 2v'_1 = \frac{1}{2h}(-5v_0 + 4v_1 + v_2), \tag{5.2a}$$

$$2v'_{m-1} + v'_m = -\frac{1}{2h}(v_{m-2} + 4v_{m-1} - 5v_m), \tag{5.2b}$$

$$v''_0 + 11v''_1 = \frac{1}{h^2}(13v_0 - 27v_1 + 15v_2 - v_3), \tag{5.2c}$$

$$11v''_{m-1} + v''_m = \frac{1}{h^2}(-v_{m-3} + 15v_{m-2} - 27v_{m-1} + 13v_m), \tag{5.2d}$$

where the prime is the partial derivative with respect to x or y. The algorithm for the nonlinear model is described in Algorithm 5.1. We remark that the iterative procedure can be applied directly to the other difference schemes as well.

Algorithm 5.1. An iterative procedure associated with the difference scheme (3.7)**.**

Step 1 Choose an initial approximation $u_{i,j}^{(0)}$ which satisfies the boundary condition.

Step 2 Compute the derivatives of the convection coefficient using (5.1a)-(5.2d).

Step 3 Solve $-\varepsilon\Delta u + u^{(0)}u_x = f$ by using scheme (3.7) to obtain $u_{i,j}^{(1)}$.

Step 4 For $k = 1,2,\cdots$, do the following steps until convergence.

Step 4.1 Set $u_{i,j}^{(k)} \leftarrow \theta u_{i,j}^{(k)} + (1-\theta)u_{i,j}^{(k-1)}$, where θ is a relaxation factor.

Step 4.2 Update the derivatives of the convection coefficient using (5.1a)-(5.2d).

Step 4.3 Solve $-\varepsilon\Delta u + u^{(k)}u_x = f$ by using scheme (3.7) to obtain $u_{i,j}^{(k+1)}$.

In our numerical simulations we take the initial approximation $u_{i,j}^{(0)}$ as

$$u_{i,j}^{(0)} = \begin{cases} \ln\left(1+\dfrac{x_i}{\varepsilon}\right) + e^{y_j}, & \text{if } (x_i, y_j) \text{ is a boundary grid point,} \\ 1, & \text{if } (x_i, y_j) \text{ is an interior grid point,} \end{cases}$$

and choose the relaxation factor $\theta = 0.8$ for all the considered schemes. All the iterative procedures are repeated until the maximum difference between successive approximations is less than 10^{-5}. The shapes of exact and numerical solutions for $\varepsilon = 10^{-2}$ are depicted in Fig. 6. Further results are reported in Table 7. When the diffusivity ε is not too small, $\varepsilon = 10^{-1}$ and 10^{-2}, the Tian-Dai scheme [24] and the Sanyasiraju-Mishra scheme [19] show a better accuracy than the others except the case of $h = 1/20$. However, when the diffusivity ε is getting small, both the above schemes lose their stability due to a large condition number at some iteration. In these cases, marked by the symbol ★ in Table 7, the estimated condition number at that iteration is approximately $\mathcal{O}(10^{10}) \sim \mathcal{O}(10^{15})$ and

Table 7: Errors in the discrete L^2-norm and the number of iteration of the numerical solutions produced by various iterative difference schemes, Example 5.5.

| ε	$1/h$	Spotz [20] Discrete L^2	Iter.	Tian-Dai [24] Discrete L^2	Iter.	S.-M. [19] Discrete L^2	Iter.	Present scheme Discrete L^2	Iter.
10^{-1}	20	8.0259e-4	9	5.6376e-4	9	2.2160e-5	9	8.0803e-4	9
	40	6.1860e-5	9	4.5479e-5	9	1.7721e-6	9	6.1860e-5	9
	80	4.0920e-6	9	3.0447e-6	9	1.4227e-7	9	4.0920e-6	9
	160	2.5822e-7	10	1.9245e-7	10	1.1609e-8	10	2.5822e-7	10
10^{-2}	20	1.7700e-1	11	★		★		1.4999e-1	10
	40	6.0852e-2	11	3.0825e-2	23	1.1594e-2	77	5.5609e-2	11
	80	1.2342e-2	11	7.0847e-3	10	4.5323e-4	10	2.1241e-2	10
	160	1.4887e-3	10	9.7372e-4	11	5.4083e-5	11	2.2440e-3	10
10^{-3}	20	6.9924e-1	11	★		★		8.8275e-1	12
	40	5.4399e-1	11	★		★		5.6387e-1	14
	80	3.7441e-1	11	★		★		3.1786e-1	15
	160	1.9021e-1	11	★		★		1.5170e-1	10
10^{-4}	20	1.3612e+0	11	★		★		2.0058e+0	14
	40	1.1119e+0	12	★		★		1.5528e+0	14
	80	8.9652e-1	13	★		★		1.1441e+0	14
	160	7.5859e-1	13	★		★		7.9630e-1	14
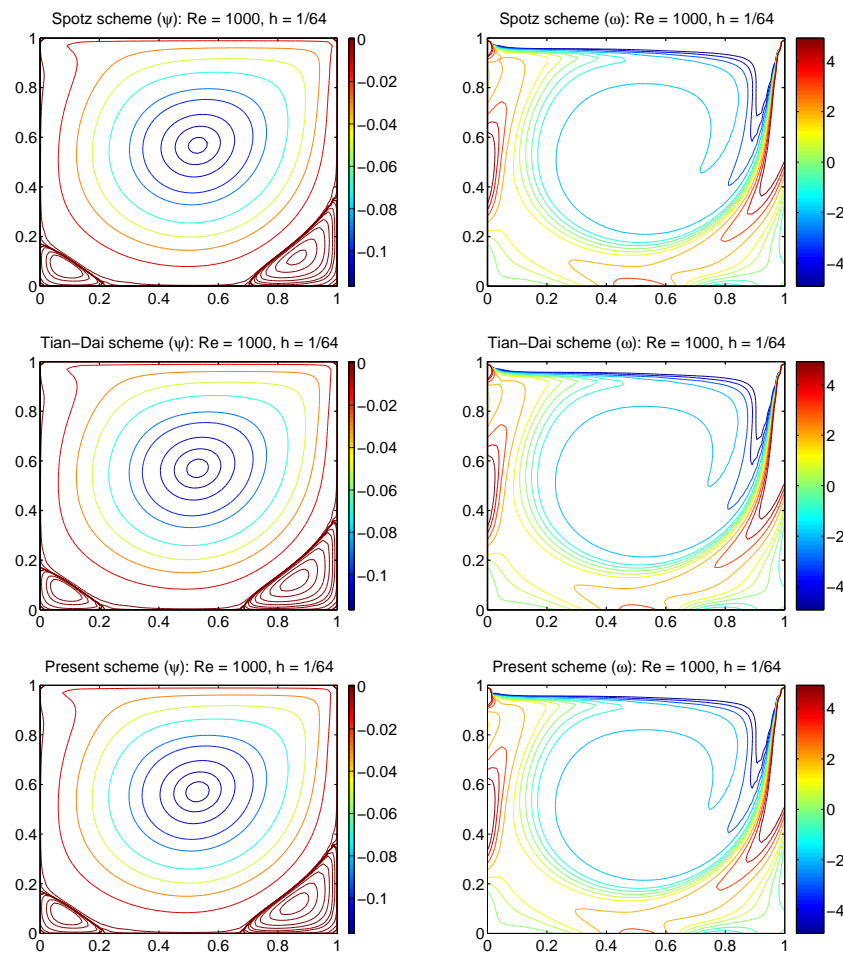
Figure 7: The contour plots of numerical solutions of Example 5.6 with $Re=1000$ and $h=1/64$.

it can not be alleviated by using other relaxation factors or initial approximations. On the other hand, at least for this example, the Spotz scheme [20] and the present difference scheme (3.7) display a better stability when the diffusivity ε is sufficiently small, but with a lower accuracy and a lower convergence rate.

Example 5.6 (The lid-driven cavity flow problem)**.** In this example, we consider the lid-driven cavity flow with $f=0$ in the unit square domain $\Omega=(0,1)\times(0,1)$. The no slip boundary condition, $u=v=0$, is applied on all boundaries except at the upper boundary where $u=1$ and $v=0$. Numerical results produced by the Spotz scheme [21], the Tian-Dai scheme [24] and the scheme (3.7) with Reynolds numbers $Re(=1/\nu)=1000, 3200, 5000$ are given in Figs. 7-9, respectively. The iterative procedure mentioned in Section 4 is repeated until the maximum difference between successive approximations of both ω and ψ are smaller than 10^{-5}. We note that the corner eddies are clearly shown in each figure. These results are also compared with the well-documented benchmark results
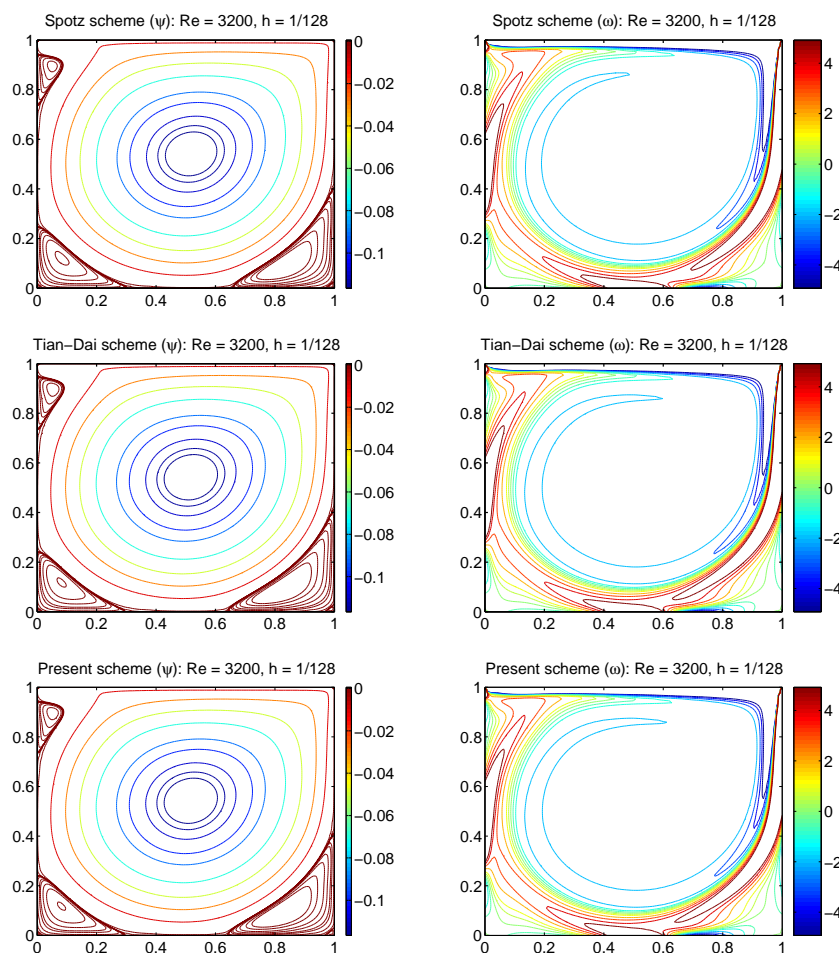
Figure 8: The contour plots of numerical solutions of Example 5.6 with $Re=3200$ and $h=1/128$.

given by Ghia-Ghia-Shin [3]. Some of the comparison is presented in Fig. 10. Apparently, the computed results of the proposed scheme (3.7) show good agreement with that of the other difference schemes.

6 Summary and conclusions

In this paper, we have proposed a high-accuracy finite difference scheme for solving reaction-convection-diffusion problems with a small diffusivity ε. With a novel treatment for the reaction term, we have first derived a three-point difference scheme for the 1-D case with accuracy of $\mathcal{O}(\varepsilon^2 h + \varepsilon h^2 + h^3)$. We have extended the scheme to the 2-D case on a nine-point stencil by using the alternating direction technique, and have showed that the difference scheme offers an accuracy of $\mathcal{O}(\varepsilon^2(h+k)+\varepsilon(h^2+k^2)+(h^3+k^3))$. Finally, the
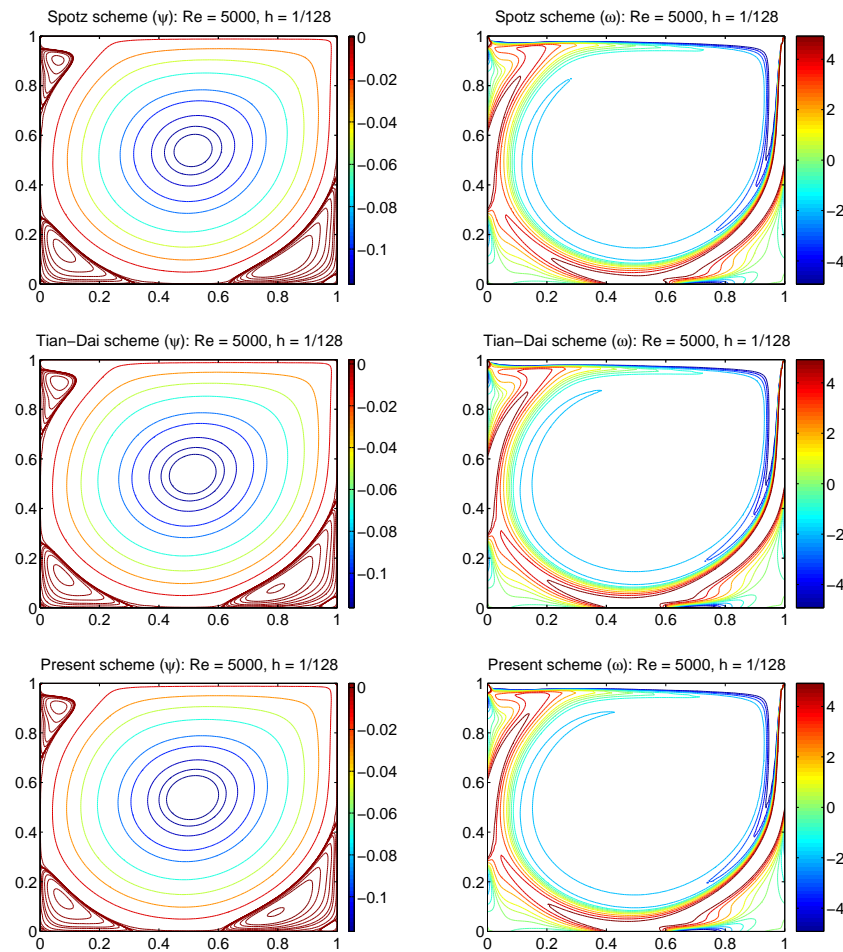
Figure 9: The contour plots of numerical solutions of Example 5.6 with $Re = 5000$ and $h = 1/128$.

proposed difference scheme was applied to solve the 2-D steady incompressible Navier-Stokes equations in the stream function-vorticity formulation. In order to demonstrate the high performance of the proposed difference scheme, we have presented a number of examples exhibiting boundary or interior layers, including the lid-driven cavity flow problem for various Reynolds numbers. The numerical results obtained were compared with those of some higher-order difference schemes in the literature. From these comparisons, we have found that our scheme can achieve good accuracy with a better stability for problems with a small diffusivity.

We conclude this paper with two brief remarks and speculation on future works. First, the underlying idea behind the proposed difference scheme may be applied to solve some coupled systems of reaction-convection-dominated equations [15]. Second, using the techniques introduced in, e.g., [1, 8, 9, 12, 25], the proposed difference scheme can be further extended to solve the unsteady reaction-convection-diffusion problems with
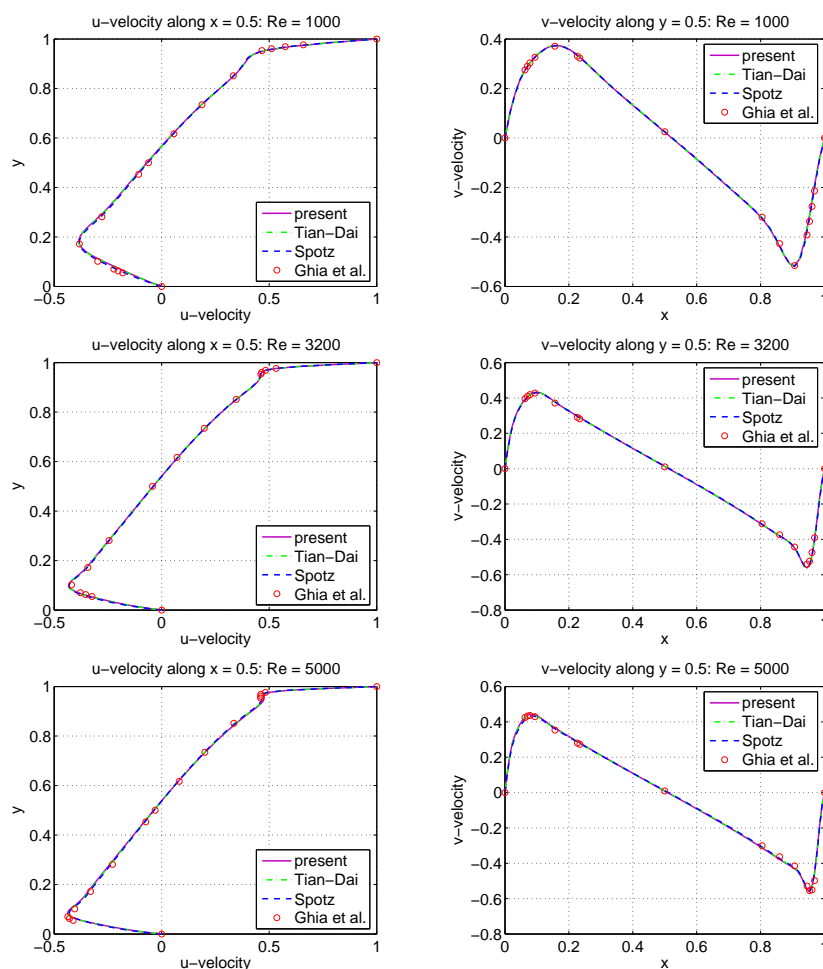
Figure 10: The profiles of numerical velocity components of Example 5.6 vs. benchmark results of Ghia-Ghia-Shin [3] for $Re = 1000, 3200, 5000$.

a small diffusivity as well as the 2-D unsteady incompressible Navier-Stokes equations in the stream function-vorticity formulation. These efforts are in progress and we will report the results in the near future.

Acknowledgments

References

[1] H. DING AND Y. ZHANG, *A new difference scheme with high accuracy and absolute stability for solving convection-diffusion equations*, J. Comput. Appl. Math., 230 (2009), pp. 600–606.

[2] H. C. ELMAN, D. J. SILVESTER AND A. J. WATHEN, Finite Elements and Fast Iterative Solvers: with Applications in Incompressible Fluid Dynamics, Oxford University Press, New York, 2005.

[3] U. GHIA, K. N. GHIA AND C. T. SHIN, *High Re-solution for incompressible Navier-Stokes equation and a multigrid method*, J. Comput. Phys., 48 (1982), pp. 387–411.

[4] M. M. GUPTA, *High accuracy solutions of incompressible Navier-Stokes equations*, J. Comput. Phys., 93 (1991), pp. 343–359.

[5] M. M. GUPTA AND J. C. KALITA, *A new paradigm for solving Navier-Stokes equations: streamfunction-velocity formulation*, J. Comput. Phys., 207 (2005), pp. 52–68.

[6] P.-W. HSIEH AND S.-Y. YANG, *Two new upwind difference schemes for a coupled system of convection-diffusion equations arising from the steady MHD duct flow problems*, J. Comput. Phys., 229 (2010), pp. 9216–9234.

[7] P.-W. HSIEH AND S.-Y. YANG, *A novel least-squares finite element method enriched with residual-free bubbles for solving convection-dominated problems*, SIAM J. Sci. Comput., 32 (2010), pp. 2047–2073.

[8] S. KARAA AND J. ZHANG, *High order ADI method for solving unsteady convection-diffusion problems*, J. Comput. Phys., 198 (2004), pp. 1–9.

[9] S. KARAA, *A hybrid Padé ADI scheme of higher-order for convection-diffusion problems*, Int. J. Numer. Meth. Fluids, 64 (2010), pp. 532–548.

[10] R. J. LEVEQUE, Finite Difference Methods for Ordinary and Partial Differential Equations, Society for Industrial and Applied Mathematics, Philadelphia, USA, 2007.

[11] M. LI, T. TANG AND B. FORNBERG, *A compact fourth-order finite difference scheme for the steady incompressibe Navier-Stokes equations*, Int. J. Numer. Meth. Fluids, 20 (1995), pp. 1137–1151.

[12] M. LI AND T. TANG, *A compact fourth-order finite difference scheme for unsteady viscous incompressible flows*, J. Sci. Comput., 16 (2001), pp. 29–45.

[13] K. MAHESH, *A family of high order finite difference schemes with good spectral resolution*, J. Comput. Phys., 145 (1998), pp. 332–358.

[14] K. W. MORTON, Numerical Solution of Convection-Diffusion Problems, Chapman & Hall, London, UK, 1996.

[15] E. O'RIORDAN AND M. STYNES, *Numerical analysis of a strongly coupled system of two singularly perturbed convection-diffusion problems*, Adv. Comput. Math., 30 (2009), pp. 101–121.

[16] A. C. RADHAKRISHNA PILLAI, *Fourth-order exponential finite difference methods for boundary value problems of convective diffusion type*, Int. J. Numer. Meth. Fluids, 37 (2001), pp. 87–106.

[17] H.-G. ROOS, M. STYNES AND L. TOBISKA, Numerical Methods for Singularly Perturbed Differential Equations, Springer, New York, 1996.

[18] Y. V. S. S. SANYASIRAJU AND N. MISHRA, *Spectral resolutioned exponential compact higher order scheme (SRECHOS) for convection-diffusion equations*, Comput. Methods Appl. Mech. Eng., 197 (2008), pp. 4737–4744.

[19] Y. V. S. S. SANYASIRAJU AND N. MISHRA, *Exponential compact higher order scheme for nonlinear steady convection-diffusion equations*, Commun. Comput. Phys., 9 (2011), pp. 897–916.

[20] W. F. SPOTZ, High-Order Compact Finite Difference Schemes for Computational Mechanics, Ph.D. Dissertation, the University of Texas at Austin, December 1995.

[21] W. F. SPOTZ, *Accuracy and performance of numerical wall boundary conditions for steady, 2D,*

incompressible streamfunction vorticity, Int. J. Numer. Meth. Fluids, 28 (1998), pp. 737–757.

[22] W. F. SPOTZ AND G. F. CAREY, *High-order compact scheme for the stream-function vorticity equations*, Int. J. Numer. Meth. Eng., 38 (1995), pp. 3497–3512.

[23] M. STYNES, *Steady-state convection-diffusion problems*, Acta Numer., (2005), pp. 445–508.

[24] Z. F. TIAN AND S. Q. DAI, *High-order compact exponential finite difference methods for convection-diffusion type problems*, J. Comput. Phys., 220 (2007), pp. 952–974.

[25] Z. F. TIAN AND Y. B. GE, *A fourth-order compact ADI method for solving two-dimensional unsteady convection-diffusion problems*, J. Comput. Appl. Math., 198 (2007), pp. 268–286.

[26] I. YAVNEH, *Analysis of a fourth-order compact scheme for convection-diffusion*, J. Comput. Phys., 133 (1997), pp. 361–364.